I2Q: A Fully Decentralized Q-Learning Algorithm

Jiechuan Jiang
Peking University
jiechuan.jiang@pku.edu.cn

Zongqing Lu[†]
Peking University
zongqing.lu@pku.edu.cn

Abstract

Fully decentralized multi-agent reinforcement learning has shown great potentials for many real-world cooperative tasks, where the global information, *e.g.*, the actions of other agents, is not accessible. Although independent Q-learning is widely used for decentralized training, the transition probabilities are non-stationary since other agents are updating policies simultaneously, which leads to non-guaranteed convergence of independent Q-learning. To deal with non-stationarity, we first introduce stationary ideal transition probabilities, on which independent Q-learning could converge to the global optimum. Further, we propose a fully decentralized method, I2Q, which performs independent Q-learning on the modeled ideal transition function to reach the global optimum. The modeling of ideal transition function in I2Q is fully decentralized and independent from the learned policies of other agents, helping I2Q be free from non-stationarity and learn the optimal policy. Empirically, we show that I2Q can achieve remarkable improvement in a variety of cooperative multi-agent tasks.

1 Introduction

Multi-agent reinforcement learning (MARL) has shown great potentials in real-world applications, including UAV [19], IoT [3], and games [28]. A number of MARL methods have been proposed for training agents to cooperatively maximize the cumulative shared reward, most of which follow the paradigm of centralized training and decentralized execution (CTDE), where the information of all agents is collected and used in the training phase. However, in many industrial applications where agents may belong to different companies, *e.g.*, autonomous vehicles or robots, the actions of other agents may not be accessible, so that CTDE methods cannot work. One way to address this challenge is *fully decentralized learning*, where the agents only use local experiences without the actions of other agents in both training and execution.

Independent Q-learning [27, 26] is one of the most straightforward decentralized methods. However, since other agents are treated as a part of the environment, from the perspective of individual agent, the transition probabilities that also depend on the policies of other agents will change as other agents are updating their policies simultaneously [7]. Whether the agent updates the individual Q-values using the off-policy experiences, which are stored in the decentralized replay buffer, or the on-policy experiences, which are collected under the latest learned policies of all agents, the transition probabilities are non-stationary, thus the convergence of independent Q-learning is not theoretically guaranteed.

To tackle the non-stationarity problem, we propose a novel variant of independent Q-learning. First, we introduce *ideal transition probabilities* for each agent, which is induced by the optimal conditional joint policy of other agents, conditioned on action of this agent. We theoretically show that if all agents independently perform Q-learning on respective ideal transition probabilities, their policies converge to the optimal joint policy when there is only one optimal joint policy. Certainly, such

[†]Corresponding Author

36th Conference on Neural Information Processing Systems (NeurIPS 2022).

ideal transition probabilities are unknown in advance, but they can be deliberately learned by each agent in a decentralized way. We let each agent learn the QSS-value [6], the value of *state* and *next state*, which will converge on its replay buffer and be equivalent with the optimal joint Q-value in deterministic environments. Then, for each agent, the next state under ideal transition probabilities, given a state and an action, is the one with the highest QSS-value. Therefore, each agent can model an ideal transition function by learning QSS value and perform independent Q-learning on the ideal transition function, which guarantees the convergence to the optimal policy.

The proposed method, ***ideal independent Q-learning*** (**I2Q**), is fully decentralized, without the information of other agents. Although the theoretical proof is built on deterministic environments, I2Q can also be applied in stochastic environments. We theoretically analyze the value gap and experimentally demonstrate its effectiveness in stochastic environments. We evaluate I2Q on a variety of multi-agent cooperative tasks, *i.e.*, matrix games, MPE-based differential games [14], Multi-Agent MuJoCo [5], and SMAC [22], covering fully and partially observable, deterministic and stochastic, discrete and continuous environments. Empirically, I2Q outperforms baselines, verifying the analyzed convergence and optimality, and the modeled ideal transition function.

2 Related Work

CTDE. Most of recent MARL methods follow the paradigm of centralized training and decentralized execution (CTDE). Policy-based methods [14, 8, 30, 34, 24, 17] extend policy-gradient into multi-agent cases by designing different optimization objectives. Value factorization methods [25, 21, 23, 29, 20] decompose the joint value function into individual value functions according to the Individual-Global-Max condition. In these methods, the information of all agents can be accessed in a centralized way during training, and the convergence can be guaranteed. Unlike these methods, we focus on decentralized learning where global information is not available.

DTDE. When agents cannot obtain the global information, they have to adopt decentralized training and decentralized execution (DTDE). The most straightforward decentralized methods are independent Q-learning [26] and independent PPO [4]. However, since all agents are updating policies simultaneously, from the perspective of each agent, the transition probabilities are non-stationary, and thus the convergence of these methods may not be guaranteed. Fingerprints [7] uses iteration number and exploration rate to alleviate the problem of obsolete experiences in replay buffer for independent Q-learning. Hysteretic-QL [15] and Lenient-QL [16] let the agents be optimistic and attach less importance to the value punishment. However, none of these variants guarantees the convergence of independent Q-learning. Some theoretical methods [2, 35] guarantee the convergence to a Nash equilibrium, but the converged equilibrium may not be the optimal one when there are multiple equilibria [32]. Moreover, there methods cannot use replay buffer and have to re-collect experiences once the policies are updated, which is not practical. Our I2Q is a practical method to learn the optimal policy using replay buffer. Some studies [33, 10] consider decentralized learning with communication. However, in our fully decentralized settings, agents cannot share any information.

3 Method

We first introduce the problem setting and analyze the non-stationarity in independent Q-learning. Then, we construct ideal transition probabilities, on which the agents are theoretically guaranteed to converge to the optimal joint policy via independent Q-learning. Finally, we propose I2Q, which performs independent Q-learning on the modeled ideal transition function.

3.1 Preliminaries

There are N agents in multi-agent MDP $M_{\text{env}} =< \mathcal{S}, \mathcal{O}, \mathcal{A}, R, P_{\text{env}}, \gamma >$ with the state space $\mathcal{S}$ and the joint action space $\mathcal{A}$. At each timestep, each agent i performs an individual action a_i, and the environment transitions to the next state s' by taking the joint action $\boldsymbol{a}$ with the transition probabilities $P_{\text{env}}\left(s'|s, \boldsymbol{a}\right)$. For simplicity of theoretical analysis, we let all agents obtain the state s [12], though in practice each agent i may learn based on the observation $o_i \in \mathcal{O}$. All agents get a shared reward $r = R\left(s, s'\right)$ and learn to maximize the expected return $\mathbb{E}\sum_{t=0}^{\infty}\gamma^t r_t$, where γ is the discount factor. We consider the fully decentralized learning, where M_{env} is partially observable to each agent since each agent only observes its own action a_i instead of the joint action $\boldsymbol{a}$. From the perspective of

each agent i, there is an MDP $M_i =< \mathcal{S}, \mathcal{A}_i, R, P_i, \gamma >$ with the individual action space $\mathcal{A}_i$ and the transition probabilities

$$P_i\left(s'|s, a_i\right) = \sum_{\boldsymbol{a}_{-i}} P_{\text{env}}\left(s'|s, \boldsymbol{a}\right) \boldsymbol{\pi}_{-i}(\boldsymbol{a}_{-i}|s), \tag{1}$$

where $\boldsymbol{a}_{-i}$ and $\boldsymbol{\pi}_{-i}$ respectively denote the joint action and the joint policy of all agents except agent i. Each agent performs independent Q-learning:

$$Q_i(s, a_i) = \mathbb{E}_{P_i(s'|s,a_i)}\left[r + \gamma \max_{a_i'} Q_i(s', a_i')\right]. \tag{2}$$

In this paper, all Q values denote the optimal values Q^*, we refer to Q^* as Q for simplicity. According to (1), the transition probabilities depend on the policies of other agents. Since other agents are updating their policies continuously, P_i becomes non-stationary during training. Concretely, if each agent i updates Q_i in an off-policy way, using the experiences stored in the replay buffer $\mathcal{D}_i$, which does not contain other agents' actions, the transition probabilities P_i in the replay buffer could be seen as the ones depending on the average policy $\bar{\boldsymbol{\pi}}_{-i}$ along the training process, which is non-stationary and outdated [7]. If each agent learns in an on-policy way, only using the most recent experiences, P_i could be seen as the one under the latest learned policy $\boldsymbol{\pi}_{-i}$, which are not outdated but still non-stationary. The convergence of Q-learning on non-stationary transition probabilities is not guaranteed. *How to solve the non-stationarity?* In the next section, we introduce ideal transition probabilities and prove that if all agents perform independent Q-learning on the ideal transition probabilities, they will converge to the optimal joint policy.

3.2 Ideal Transition Probabilities

Assume there is only one optimal joint policy $\boldsymbol{\pi}^*(s) = \arg\max_{\boldsymbol{a}} Q(s, \boldsymbol{a})$, where Q is the optimal joint Q-function,

$$Q(s, \boldsymbol{a}) = \mathbb{E}_{P_{\text{env}}(s'|s,\boldsymbol{a})}\left[r + \gamma \max_{\boldsymbol{a}'} Q(s', \boldsymbol{a}')\right]. \tag{3}$$

The unique optimal policy $\boldsymbol{\pi}^*(s)$ must be deterministic [18]. Thus, $\boldsymbol{\pi}^*$ can be uniquely factorized into deterministic optimal individual policies $\boldsymbol{\pi}^* = \langle \pi_1^*, \pi_2^*, \cdots, \pi_N^* \rangle$. For agent i, we build a deterministic optimal joint policy of other agents which is conditioned on a_i:

$$\boldsymbol{\pi}_{-i}^*(s, a_i) = \arg\max_{\boldsymbol{a}_{-i}} Q(s, a_i, \boldsymbol{a}_{-i}). \tag{4}$$

There may exist multiple $\boldsymbol{\pi}_{-i}^*$, and we can choose one arbitrarily. If other agents act the policy $\boldsymbol{\pi}_{-i}^*(s, a_i)$, the transition probabilities viewed by agent i is $P_i\left(s'|s, a_i\right) = P_{\text{env}}\left(s'|s, a_i, \boldsymbol{\pi}_{-i}^*(s, a_i)\right)$, which are defined as ***ideal transition probabilities***. Then we have the following theorem.

Theorem 1. *If agent i performs Q-learning on the ideal transition probabilities $P_i\left(s'|s, a_i\right) = P_{\text{env}}\left(s'|s, a_i, \boldsymbol{\pi}_{-i}^*(s, a_i)\right)$, its policy will converge to the optimal individual policy π_i^*.*

Proof. According to the fixed-point formulation of Q-learning, we have

$$Q_i(s, a_i) = \mathbb{E}_{P_{\text{env}}\left(s'|s,a_i,\boldsymbol{\pi}_{-i}^*(s,a_i)\right)}\left[r + \gamma \max_{a_i'} Q_i(s', a_i')\right], \tag{5}$$

$$\max_{\boldsymbol{a}_{-i}} Q(s, a_i, \boldsymbol{a}_{-i}) = \max_{\boldsymbol{a}_{-i}} \mathbb{E}_{P_{\text{env}}(s'|s,\boldsymbol{a})}\left[r + \gamma \max_{a_i'} \max_{\boldsymbol{a}_{-i}'} Q(s, a_i', \boldsymbol{a}_{-i}')\right] \tag{6}$$

$$= \mathbb{E}_{P_{\text{env}}\left(s'|s,a_i,\boldsymbol{\pi}_{-i}^*(s,a_i)\right)}\left[r + \gamma \max_{a_i'} \max_{\boldsymbol{a}_{-i}'} Q(s, a_i', \boldsymbol{a}_{-i}')\right], \tag{7}$$

where (6) is from taking $\max_{\boldsymbol{a}_{-i}}$ on both sides of (3), and (7) is by folding $\max_{\boldsymbol{a}_{-i}}$ into P_{env}. From (5) and (7), we see $Q_i(s, a_i)$ and $\max_{\boldsymbol{a}_{-i}} Q(s, a_i, \boldsymbol{a}_{-i})$ have the same stationary Bellman operator. According to the contraction mapping theorem, the Bellman operator converges to a unique fixed point. Thus,

$$Q_i(s, a_i) = \max_{\boldsymbol{a}_{-i}} Q(s, a_i, \boldsymbol{a}_{-i}).$$

Then, we have:

$$\max_{a_i} Q_i(s, a_i) = \max_{a_i} \max_{\boldsymbol{a}_{-i}} Q(s, a_i, \boldsymbol{a}_{-i}) = Q(s, \boldsymbol{\pi}^*(s)). \tag{8}$$

By contradiction, if an $\tilde{a}_i \neq \pi_i^*(s)$ but satisfies $Q_i(s, \tilde{a}_i) \geq Q_i(s, \pi_i^*(s)) = Q(s, \boldsymbol{\pi}^*(s))$, it contradicts that $\boldsymbol{\pi}^*$ is the unique optimal joint policy. Therefore, $\pi_i^*(s) = \arg\max Q_i(s, a_i)$. □

By extending this theorem, if all agents perform Q-learning on such ideal transition probabilities under the conditional optimal joint policy, they will converge to the respective optimal individual policies, and arrive at the optimal joint policy $\langle \pi_1^*, \pi_2^*, \cdots, \pi_N^* \rangle$.

3.3 I2Q

How to obtain the ideal transition probabilities from the non-stationary replay buffer for each agent? We first introduce the QSS-learning [6]. Following the setting of QSS [6], we assume the environment is deterministic.[1] Each agent i learns a value function $Q_i^{\text{ss}}(s, s')$ using the experiences in its own replay buffer $\mathcal{D}_i$:

$$Q_i^{\text{ss}}(s, s') = r + \gamma \max_{s'' \in \mathcal{N}(s')} Q_i^{\text{ss}}(s', s''), \tag{9}$$

where $\mathcal{N}(s')$ is the neighboring state set of the state s' (the set of all next states of s'). The value function Q_i^{ss} has several advantages. First, it has been proven in QSS [6] that Q_i^{ss} and Q learn equivalent values, which means

$$\max_{s'} Q_i^{\text{ss}}(s, s') = \max_{\boldsymbol{a}} Q(s, \boldsymbol{a}). \tag{10}$$

The equivalence shows that agent i can independently infer the next state under the optimal joint policy according to $\arg\max_{s'} Q_i^{\text{ss}}(s, s')$. Second, as $Q_i^{\text{ss}}(s, s')$ decouples the action a_i from the value and the implied transition probabilities: $P(s'|s, s') = 1, \forall s' \in \mathcal{N}(s)$, are always stationary, Q_i^{ss} converges to the optimal value even on its own replay buffer, without the information of other agents. Third, since all agents act in the same environment, they collect the same states set and the same next state set in their own replay buffers. Therefore, they will converge to the same Q_i^{ss} independently, which builds the consensus between the learned policies of agents.

Then, how to build the ideal transition function from Q_i^{ss}? As the environment P_{env} and the optimal conditional joint policy of other agents $\boldsymbol{\pi}_{-i}^*(s, a_i)$ are deterministc, under the ideal transition probabilities $P_{\text{env}}\left(s'|s, a_i, \boldsymbol{\pi}_{-i}^*(s, a_i)\right)$, the environment from the perspective of agent i will deterministically transition to the next state that has the highest Q_i^{ss} among all neighboring states given a_i:

$$s'^* = \arg\max_{s' \in \mathcal{N}(s, a_i)} Q_i^{\text{ss}}(s, s'), \tag{11}$$

where $\mathcal{N}(s, a_i)$ is the neighboring state set of s given a_i. This is proved in the proof of the following theorem.

Theorem 2. *In deterministic environments, all agents will converge to the optimal policies, if each agent i performs Q-learning on the transition function $s'^* = \arg\max_{s' \in \mathcal{N}(s, a_i)} Q_i^{\text{ss}}(s, s')$.*

Proof. The proof is given in Appendix A, which shows that $s'^* = \arg\max_{s' \in \mathcal{N}(s, a_i)} Q_i^{\text{ss}}(s, s')$ is the ideal transition function. □

To model the stationary ideal transition function $s'^* = \arg\max_{s' \in \mathcal{N}(s, a_i)} Q_i^{\text{ss}}(s, s')$, we train a neural network $f_i(s, a_i)$ to predict s'^* and update $f_i(s, a_i)$ by maximizing:

$$\mathbb{E}_{s, a_i, s' \sim \mathcal{D}_i}\left[\lambda Q_i^{\text{ss}}(s, f_i(s, a_i)) - (f_i(s, a_i) - s')^2\right]. \tag{12}$$

The first term enforces that the predicted next state has the highest Q_i^{ss}, and the second term constrains the predicted next state to be in the set $\mathcal{N}(s, a_i)$. The hyperparameter λ is the coefficient. Based on the transition model $f_i(s, a_i)$, Q_i^{ss} is updated by minimizing the TD-error:

$$\mathbb{E}_{s, a_i, s', r \sim \mathcal{D}_i}\left[\left(Q_i^{\text{ss}}(s, s') - r - \gamma \bar{Q}_i^{\text{ss}}(s', f_i(s', a_i'^*))\right)^2\right], \quad a_i'^* = \arg\max_{a_i'} Q_i(s', a_i'). \tag{13}$$

[1] Although the environment P_{env} is deterministic, from the perspective of each agent i, the viewed environment P_i would still be non-stationary.

Algorithm 1. I2Q for each agent i

Initialize transition model f_i, Q-networks Q_i and Q_i^{ss}, and the target networks $\bar{Q}_i$ and $\bar{Q}_i^{\text{ss}}$.
Initialize the replay buffer $\mathcal{D}_i$.
for $t = 1, \ldots, max_iteration$ **do**
  All agents interact in the environment and store experiences (s, a_i, s', r) in replay buffer $\mathcal{D}_i$.
  Sample a mini-batch from $\mathcal{D}_i$.
  Update f_i by maximizing (12).
  Update Q_i^{ss} by minimizing (13).
  Update Q_i by minimizing (14) or (15).
  Update the target networks $\bar{Q}_i$ and $\bar{Q}_i^{\text{ss}}$.
end for

And Q_i is updated by minimizing:

$$\mathbb{E}_{s,a_i,r\sim\mathcal{D}_i}\left[\left(Q_i\left(s,a_i\right) - r - \gamma \max_{a_i'} \bar{Q}_i(f_i(s,a_i), a_i')\right)^2\right]. \tag{14}$$

$\bar{Q}$ is the target network of Q. When updating Q_i (14), the target value is not computed on the next state sampled from replay buffer D_i, but on the one predicted by the modeled ideal transition function $f_i(s, a_i)$. In (14), the reward r is simplified to depending just on s. When r depends on both s and s', given s and a_i, the next state under the ideal transition function (11) satisfies:

$$\begin{aligned} Q_i^{\text{ss}}(s, s'^*) &= r(s, s'^*) + \gamma \max_{s''} Q_i^{\text{ss}}(s'^*, s'') \\ &= r(s, s'^*) + \gamma \max_{\boldsymbol{a}'} Q(s'^*, \boldsymbol{a}') \leftarrow (10) \\ &= r(s, s'^*) + \gamma \max_{a_i'} Q_i(s'^*, a_i') \leftarrow (8) \\ &= Q_i(s, a_i) \leftarrow (\text{deterministic ideal transition probabilities}). \end{aligned}$$

Therefore, we can update Q_i by minimizing:

$$\mathbb{E}_{s,a_i\sim\mathcal{D}_i}\left[\left(Q_i\left(s,a_i\right) - \bar{Q}_i^{\text{ss}}(s, f_i(s,a_i)\right)^2\right]. \tag{15}$$

The training procedure of I2Q is summarize in Algorithm 1, where each agent i learns f_i, Q_i^{ss}, and Q_i. Although all the modules update simultaneously, as the convergence of Q_i^{ss} is guaranteed, the transition function f_i derived from Q_i^{ss} will be stationary in the later stage. Thus Q_i will also converge. I2Q can be applied in environments with both discrete and continuous state-action space. In continuous action space, we build I2Q on DDPG [13], where a policy network $\pi_i(s)$ is trained by maximizing $Q_i(s, \pi_i(s))$ as a substitute of $\arg\max_{a_i} Q_i(s, a_i)$. In continuous state space, since $f_i(s, a_i)$ is differentiable, (12) can be maximized by gradient ascent. In discrete state space or large state space, we can map the state space to a continuous embedding space, and apply I2Q on the embedding space. We also provide an implemetation without forward model f_i in Appendix B.7.

3.4 Assumptions

We will further discuss the two assumptions. The prime one is that there is only one optimal joint policy, but I2Q can easily solve tasks with multiple optimal joint policies. With multiple optimal actions (with the max $Q_i(s, a_i)$), if each agent arbitrarily selects one of the optimal independent actions, the joint action might not be the optimal. To address this, we can set a performance tolerance ε and introduce a fixed randomly initialized reward function $\hat{r}(s, s')$ in the range $(0, \hat{r}_{\max}]$, where $\hat{r}_{\max} = (1-\gamma)\varepsilon$. Then all agents perform I2Q on the shaped reward $r + \hat{r}$ and learn the value function $\hat{Q}_i(s, a_i)$ in terms of of $r + \hat{r}$. Since $\hat{r}$ is positive, $\hat{Q}_i(s, a_i) > Q_i(s, a_i)$. In $\hat{Q}_i(s, a_i)$, the maximal contribution from $\hat{r}$ is $\hat{r}_{\max}/(1-\gamma) = \varepsilon$, so the minimal contribution from r is $\hat{Q}_i(s, a_i) - \varepsilon > Q_i(s, a_i) - \varepsilon$, which means that the maximal performance drop is ε when selecting actions according to $\hat{Q}_i$. Moreover, since the reward function $\hat{r}(s, s')$ is randomly initialized, it is a small probability event to find multiple optimal joint policies on the reward function $r + \hat{r}$. Thus, if ε is set to be small enough, I2Q could solve the task with multiple optimal joint policies.

The secondary one is deterministic environments. In stochastic environments, (10) does not hold, and $Q_i^{\text{ss}}(s, s')$ can be considered the "best possible value" [6]. So $s'^* = \arg\max_{s'\in\mathcal{N}(s,a_i)} Q_i^{\text{ss}}(s, s')$ is

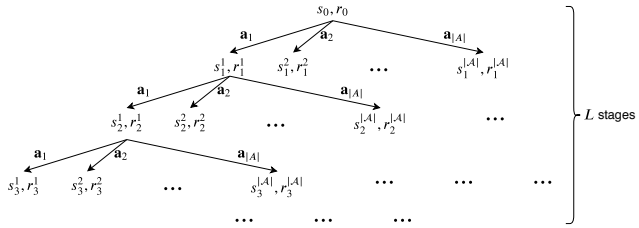

Figure 1: Illustration of the matrix games.

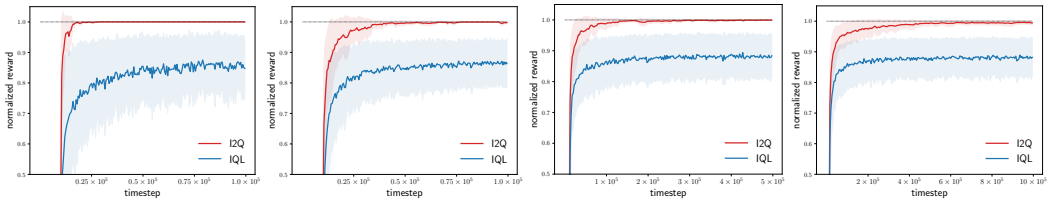

(a) $L = 3$ (b) $L = 4$ (c) $L = 5$ (d) $L = 6$

Figure 2: Learning curves on 100 random matrix games with different stage L.

the best possible transition function, rather than the ideal transition function. The difference between the learned Q_i of I2Q and the true value under the ideal transition function Q_i^{sto} is guaranteed by the following theorem.

Theorem 3. $\|Q_i^{sto} - Q_i\|_\infty \leq \frac{\Delta r}{1-\gamma} \left\| \frac{1-P_{\text{env}}\left(s'^*|s,a_i,\boldsymbol{\pi}^*_{-i}(s,a_i)\right)}{1-\gamma P_{\text{env}}\left(s'^*|s,a_i,\boldsymbol{\pi}^*_{-i}(s,a_i)\right))} \right\|_\infty$, *where* $\Delta r = r_{\max} - r_{\min}$.

Proof. The proof is given in Appendix A. □

Theorem 3 shows that Q_i of I2Q is closer to the true value if the transition probability of s'^* is higher in stochastic environments. Since we sample transitions from $\mathcal{D}_i$ to update f_i by maximizing (12), the second term of (12) makes the predicted next state $f_i(s, a_i)$ be close to the ***high-frequency*** next states in replay buffer $\mathcal{D}_i$ given s and a_i, which means that the transition probability of the predicted next state $P_{\text{env}}\left(f_i(s, a_i)|s, a_i, \boldsymbol{\pi}^*_{-i}(s, a_i)\right)$ would not be too small. Thus, Q_i of I2Q will be close to the true value and the worst cases where the predicted next states have very small transition probabilities can be avoided. ***That is the reason why I2Q can be successfully applied in stochastic environments***

4 Experiments

In experiments, we first evaluate I2Q on a class of randomly generated matrix games to verify our theoretical analysis. Second, we compare I2Q with a series of Q-learning variants on MPE-based [14] differential games to illustrate the convergence and optimality of I2Q on more complex tasks with continuous action. Third, we test I2Q on two popular MARL benchmarks: Multi-Agent MuJoCo [17] and SMAC [22]. The experiments cover both fully and partially observable, deterministic and stochastic, discrete and continuous environments. Since we consider the fully decentralized settings, I2Q and the baselines *do not use parameter-sharing*. The results are presented using mean and standard deviation (std) with different random seeds. More details about hyperparameters are available in Appendix C.

4.1 Matrix Games

To support the theoretical analysis of I2Q, we perform experiments on a class of two-agent matrix games with L stages. The action space of each agent is 3, so the joint action space $|\mathcal{A}| = 9$. The payoff tree is shown in Figure 1, where the reward r is randomly generated in the range $[-1, 1]$ and fixed in each matrix game. Without loss of generality, we randomly generate 100 matrix games for each stage L, train the agents for four different seeds in each game, and plot the mean normalized return (normalized by the optimal return) and std over the 100 matrix games. Since the states are countable, we adopt Q-tables instead of neural networks, where Q_i table and Q_i^{ss} table are updating *simultaneously*, and use ϵ-greedy policies. Figure 2 show the learning curves with different stages L under $\epsilon = 0.5$. IQL cannot converge to the optimal policies and shows large std, because it is afflicted

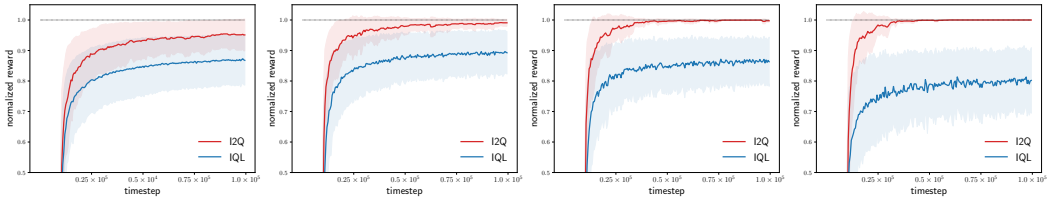

(a) $\epsilon = 0.1$ (b) $\epsilon = 0.3$ (c) $\epsilon = 0.5$ (d) $\epsilon = 0.7$

Figure 3: Learning curves with different ϵ on 100 random matrix games with stage L.

a_2 \ a_1	$\mathcal{A}^{(1)}$	$\mathcal{A}^{(2)}$	$\mathcal{A}^{(3)}$
$\mathcal{A}^{(1)}$	**8**	-12	-12
$\mathcal{A}^{(2)}$	-12	0	0
$\mathcal{A}^{(3)}$	-12	0	0

(a) case 1

a_2 \ a_1	$\mathcal{A}^{(1)}$	$\mathcal{A}^{(2)}$	$\mathcal{A}^{(3)}$
$\mathcal{A}^{(1)}$	**8**	-12	-12
$\mathcal{A}^{(2)}$	-12	6	0
$\mathcal{A}^{(3)}$	-12	0	6

(b) case 2

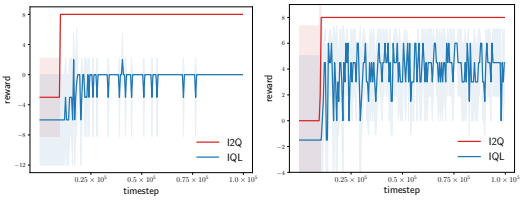

(c) curves on case 1 (d) curves on case 2

Figure 4: Learning curves on two specific one-stage matrix games.

with non-stationarity. I2Q converges to the global optimum on the matrix games, even when the stage L grows, which confirms our theoretical analysis.

In Figure 3, we show the effect of exploration rate ϵ on the matrix games with $L = 4$. As ϵ increases, I2Q converges faster, while the performance of IQL drops. In conventional decentralized methods like IQL, there is a *dilemma of exploration and exploitation*. If ϵ is small, the weak exploration causes low sample efficiency and slow learning. When ϵ is large, all agents act more randomly. From the perspective of individual agent, the transition probabilities will be much different from the real ones under the learned policies of other agents, which causes bad performance. That is the reason why IQL drops when ϵ increases. I2Q can avoid the dilemma, because $Q_i^{\text{ss}}(s, s')$ is independent from agent policies and converges faster with larger ϵ as it sees more states. Thus, I2Q can use large ϵ, *e.g.*, 0.5 or 0.7, to promote sample efficiency.

Moreover, we test I2Q on two one-stage matrix games proposed in QTRAN [23] and QPLEX [29] as shown in Figure 4, which are special cases of Figure 1. In case 1, IQL converges to the local optimum, and in case 2, IQL does not converge. Our I2Q can converge to the global optimum easily, in a fully decentralized way.

4.2 MPE

To investigate the effectiveness of I2Q in complex continuous environments with neural network implementation, we design a class of MPE-based differential games, where N agents can move in the range $[-1, 1]$. In each timestep, agent i acts the action $a_i \in [-1, 1]$, and the position of agent i is updated as $x_i = \text{clip}(x_i + 0.1 \times a_i, -1, 1)$ (*i.e.*, the updated position is clipped to $[-1, 1]$). The state is the position vector $\{x_1, x_2, \cdots, x_N\}$. The reward function of each timestep is defined as

$$r = \begin{cases} 0.5\cos(l\pi/m) + 0.5 & \text{if } l \leq m \\ 0 & \text{if } m < l \leq 0.6 \\ 0.15\cos(5\pi(l - 0.8)) + 0.15 & \text{if } 0.6 < l \leq 1.0 \\ 0 & \text{if } l > 1.0 \end{cases}, \quad l = \sqrt{\frac{2}{N}\sum_{i=0}^{N} x_i^2}, \quad m = 0.13(N-1).$$

The visualization of reward function of two-agent case is shown in Figure 5a. There is only one global optimum ($l = 0$ and $r = 1$) but infinite sub-optimum ($l = 0.8$ and $r = 0.3$), and the region with $r > 0.3$ is very narrow and surrounded by the region with $r = 0$. So it is hard to learn the optimal policies in a decentralized way. The episode contains 100 timesteps, and the agents' positions are randomly initialized at the beginning of each episode. To verify the scalability, we test I2Q in the settings with different agent numbers N, and train the agents for eight random seeds in each setting. The results are shown in Figure 6. IDDPG always falls into local optimum due to the non-stationarity and outdated transition probabilities. To be optimistic towards the value punishment is an important technique in decentralized MARL. Although adopting the optimistic update, Hysteretic IDDPG [15] still falls into local optimum due to the non-stationarity problem. D3G [6] applies the idea

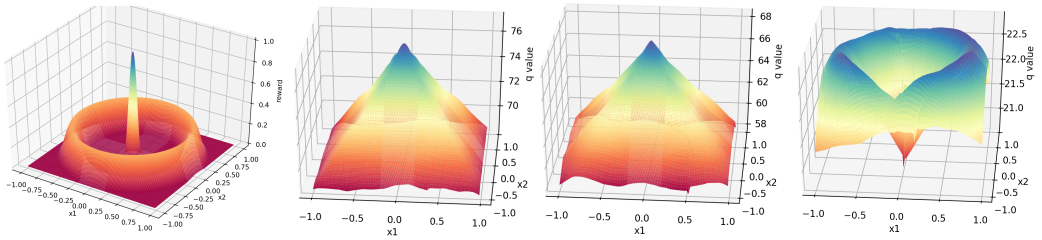

(a) reward function (b) Ideal (c) I2Q (d) IDDPG

Figure 5: (a): Visualization of reward function in differential game with two agents. (b)-(d): Visualizations of learned values of agent 1 in differential game with two agents. x1-axis and x2-axis: agents 1 and 2's positions, respectively.

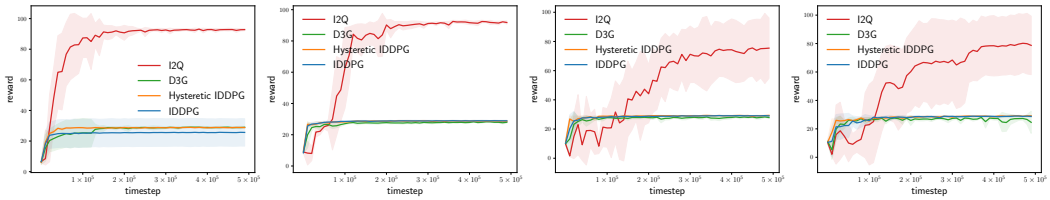

(a) $N = 2$ (b) $N = 3$ (c) $N = 4$ (d) $N = 5$

Figure 6: Learning curves on MPE-based differential games with different agent numbers N.

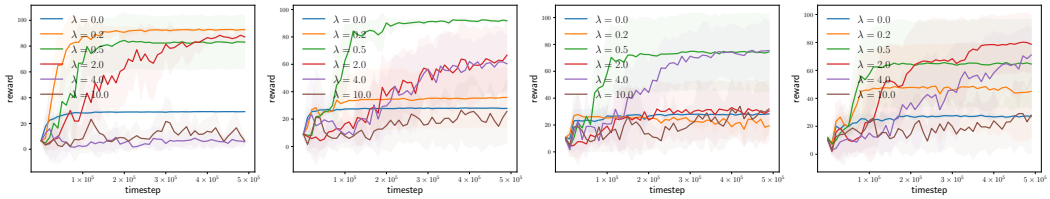

(a) $N = 2$ (b) $N = 3$ (c) $N = 4$ (d) $N = 5$

Figure 7: Learning curves on MPE-based differential games with different λ.

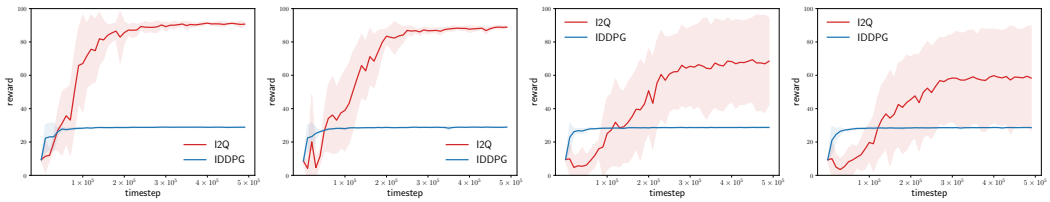

(a) $\xi = 0.02$ (b) $\xi = 0.03$ (c) $\xi = 0.04$ (d) $\xi = 0.05$

Figure 8: Learning curves on MPE-based differential games with different noise ξ.

of QSS in single-agent learning. To extend D3G into decentralized MARL, we train each agent independently using D3G, without the information of other agents. However, D3G cannot learn the optimal solution either, since the forward model in D3G requires the transition probabilities P_i to be deterministic. However, when learning on the decentralized replay buffer, P_i is the average of non-stationary transition probabilities and cannot be deterministic. Thus, D3G is not applicable to decentralized multi-agent learning. Learning on the ideal transition function inferred from $Q_i^{\text{ss}}(s, s')$, I2Q can escape from local optimum and significantly outperform others. To thoroughly demonstrate the effectiveness of I2Q, in Figure 5, we visualize the learned values of agent 1 in the two-agent case. In Figure 5b, we let the agent 2 always act the optimal policy (moving to the position $x_2 = 0$), which means the agent 1 performs Q-learning on the true ideal transition probabilities. Thus, Figure 5b shows the optimal values under ideal transition probabilities. In Figure 5c, both agents use I2Q. I2Q values are very similar to the true ideal values, where the value of the center point ($l = 0$) is the highest, which means that the modeled transition function in I2Q is close to the true one. In Theorem 4 (see Appendix A), we theoretically analyze that the difference between ideal values (Figure 5b) and I2Q values (Figure 5c) is bounded by the model error. In Figure 5d, both agents use IQL, resulting in that the value of center point ($l = 0$) is the lowest and the suboptimal points ($l = 0.8$) have the highest values.

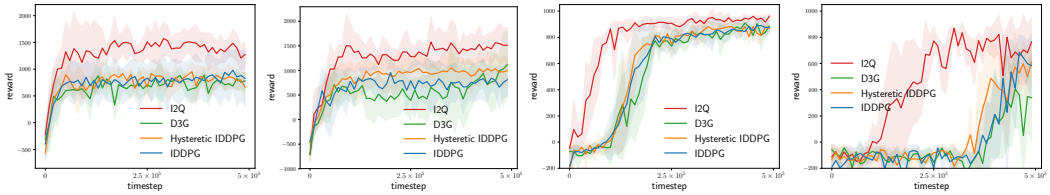

(a) 2×3 HalfCheetah (b) $2|4$ HalfCheetah (c) 2×4 Ant (d) $6|2$ Ant

Figure 9: Learning curves on Multi-Agent MuJoCo.

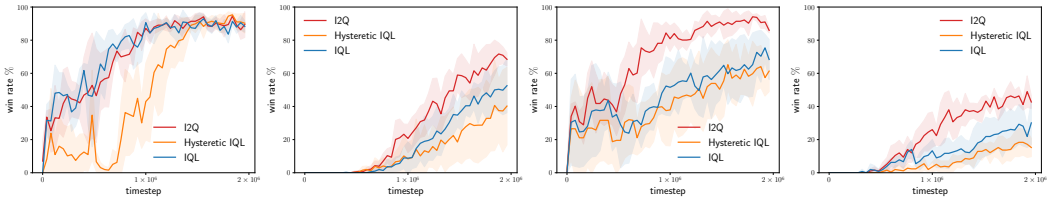

(a) 8m (b) 3s_vs_4z (c) 2s3z (d) 5m_vs_6m

Figure 10: Learning curves on SMAC.

To model the ideal transition function, next states predicted by f_i should have the highest Q_i^{ss} values (optimality) and be in the neighboring state set given state-action pair (referred to as neighborhood constraint). To achieve this objective, λ in (12) controls the balance between optimality and neighborhood constraint. Figure 7 shows the effect of λ. When λ is too small, the next state predicted by f_i cannot maximize $Q_i^{\text{ss}}(s, s')$, and thus I2Q gets stuck at local optimum. Especially, when $\lambda = 0$, I2Q degrades into a popular model-based method MBPO [9]. When λ is too large, *e.g.*, $\lambda = 10$, paying much more attention to maximize $Q_i^{\text{ss}}(s, s')$, f_i would generate out-of-neighborhood states, causing that I2Q even cannot converge to local optimum. We notice that $\lambda = 0.5$ can generally achieve a good performance in different settings of N.

Although we assume deterministic environments in theoretical analysis, I2Q can also obtain performance gain in stochastic environments. To measure the impact of stochastic environments, we add a noise to the position update: $x_i = \text{clip}(x_i + 0.1 \times a_i + \xi \times z, -1, 1)$, where z is a uniform random variable in $[-1, 1]$, and ξ is a constant controlling the randomness. Figure 8 shows the performance with different ξ in the three-agent case. In the stochastic environments, IDDPG still converges to local optimum, while I2Q always escapes from local optimum when $\xi = 0.02$ and 0.03, free from the impact of stochastic environments. When $\xi = 0.04$ and 0.05, the effect of stochasticity is nearly half of the effect of action. I2Q cannot always learn optimal policies with the strong stochasticity but still significantly outperforms IDDPG.

4.3 Multi-Agent MuJoCo and SMAC

To investigate the effectiveness of I2Q in *partially observable* environments, we perform experiments on Multi-Agent MuJoCo [17], where each agent independently controls one or some joints of the robot and could only observe the state of its own joints and bodies (with the parameter agent_obsk = 0). The results are shown in Figure 9 with eight random seeds. I2Q achieves higher reward than IDDPG, which indicates that I2Q could be extended to partially observable tasks and obtain performance gain by performing Q-learning on ideal transition probabilities instead of transition probabilities in replay buffer. In the partially observable setting, we only consider two-agent cases. When there are more agents, each agent can only control one or two joints, and the observation range is too limited to learn strong policies. In Appendix B.4, we provide the 6-agent Walker and 8-agent Ant experiments with full observation setting to verify the scalability.

We test I2Q on *partially observable and stochastic* SMAC tasks [22] with the version SC2.4.10, including both easy and hard maps [31]. We adopt the implementation of PyMARL [22] that takes as input the trajectory of partial observations, which is high-dimensional and not differentiable on some dimensions, meaning that directly optimizing (12) is hard. So the QSS model Q_i^{ss} is not built on the trajectory of partial observations, but on the hidden state of Q_i (the output of RNN layer), which is 64-dimension and differentiable, and the transition function f_i predicts the next hidden state. We train the agents for four random seeds. D3G can only be used in continuous action space, so we do

not compare with it in SMAC. As shown in Figure 10, I2Q is capable of handling high-dimensional and stochastic tasks.

5 Conclusion

We propose I2Q, a novel variant of independent Q-learning, to deal with the non-stationarity in decentralized MARL. I2Q models the ideal transition function, which depend on the optimal conditional joint policy of other agents and performs independent Q-learning on the modeled ideal transition function. Theoretically, we prove that I2Q converges to the optimal joint policy in deterministic environments. Empirically, I2Q obtains performance gain in a variety of multi-agent tasks.

Acknowledgments and Disclosure of Funding

This work was supported in part by NSF China under grant 61872009. The authors would like to thank the anonymous reviewers for their valuable comments.

References

[1] Joshua Achiam. Spinning Up in Deep Reinforcement Learning. 2018.

[2] Natalia Akchurina. Multiagent reinforcement learning: algorithm converging to nash equilibrium in general-sum discounted stochastic games. In *Proceedings of The 8th International Conference on Autonomous Agents and Multiagent Systems-Volume 2*, pages 725–732. Citeseer, 2009.

[3] Zilong Cao, Pan Zhou, Ruixuan Li, Siqi Huang, and Dapeng Wu. Multiagent deep reinforcement learning for joint multichannel access and task offloading of mobile-edge computing in industry 4.0. *IEEE Internet of Things Journal*, 7(7):6201–6213, 2020.

[4] Christian Schroeder de Witt, Tarun Gupta, Denys Makoviichuk, Viktor Makoviychuk, Philip HS Torr, Mingfei Sun, and Shimon Whiteson. Is Independent Learning All You Need in The StarCraft Multi-Agent Challenge? *arXiv preprint arXiv:2011.09533*, 2020.

[5] Christian Schroeder de Witt, Bei Peng, Pierre-Alexandre Kamienny, Philip Torr, Wendelin Böhmer, and Shimon Whiteson. Deep Multi-Agent Reinforcement Learning for Decentralized Continuous Cooperative Control. *arXiv preprint arXiv:2003.06709*, 2020.

[6] Ashley Edwards, Himanshu Sahni, Rosanne Liu, Jane Hung, Ankit Jain, Rui Wang, Adrien Ecoffet, Thomas Miconi, Charles Isbell, and Jason Yosinski. Estimating q (s, s') with deep deterministic dynamics gradients. In *International Conference on Machine Learning (ICML)*, 2020.

[7] Jakob Foerster, Nantas Nardelli, Gregory Farquhar, Triantafyllos Afouras, Philip HS Torr, Pushmeet Kohli, and Shimon Whiteson. Stabilising Experience Replay for Deep Multi-Agent Reinforcement Learning. In *International Conference on Machine Learning (ICML)*, 2017.

[8] Shariq Iqbal and Fei Sha. Actor-Attention-Critic for Multi-Agent Reinforcement Learning. In *International Conference on Machine Learning (ICML)*, 2019.

[9] Michael Janner, Justin Fu, Marvin Zhang, and Sergey Levine. When to trust your model: Model-based policy optimization. *Advances in Neural Information Processing Systems (NeurIPS)*, 2019.

[10] Sachin G Konan, Esmaeil Seraj, and Matthew Gombolay. Iterated reasoning with mutual information in cooperative and byzantine decentralized teaming. In *International Conference on Learning Representations (ICLR)*, 2021.

[11] Ilya Kostrikov, Ashvin Nair, and Sergey Levine. Offline reinforcement learning with implicit q-learning. In *International Conference on Learning Representations (ICLR)*, 2021.

[12] Jakub Grudzien Kuba, Ruiqing Chen, Munning Wen, Ying Wen, Fanglei Sun, Jun Wang, and Yaodong Yang. Trust region policy optimisation in multi-agent reinforcement learning. *International Conference on Learning Representations (ICLR)*, 2022.

[13] Timothy P Lillicrap, Jonathan J Hunt, Alexander Pritzel, Nicolas Heess, Tom Erez, Yuval Tassa, David Silver, and Daan Wierstra. Continuous control with deep reinforcement learning. In *International Conference on Learning Representations (ICLR)*, 2016.

[14] Ryan Lowe, Yi Wu, Aviv Tamar, Jean Harb, Pieter Abbeel, and Igor Mordatch. Multi-Agent Actor-Critic for Mixed Cooperative-Competitive Environments. *Neural Information Processing Systems (NeurIPS)*, 2017.

[15] Laëtitia Matignon, Guillaume J Laurent, and Nadine Le Fort-Piat. Hysteretic q-learning: an algorithm for decentralized reinforcement learning in cooperative multi-agent teams. In *2007 IEEE/RSJ International Conference on Intelligent Robots and Systems*, pages 64–69. IEEE, 2007.

[16] Gregory Palmer, Karl Tuyls, Daan Bloembergen, and Rahul Savani. Lenient Multi-Agent Deep Reinforcement Learning. In *International Conference on Autonomous Agents and MultiAgent Systems (AAMAS)*, 2018.

[17] Bei Peng, Tabish Rashid, Christian Schroeder de Witt, Pierre-Alexandre Kamienny, Philip Torr, Wendelin Böhmer, and Shimon Whiteson. Facmac: Factored multi-agent centralised policy gradients. *Advances in Neural Information Processing Systems (NeurIPS)*, 2021.

[18] Martin L Puterman. Markov decision processes: Discrete stochastic dynamic programming, 1994.

[19] Han Qie, Dianxi Shi, Tianlong Shen, Xinhai Xu, Yuan Li, and Liujing Wang. Joint optimization of multi-uav target assignment and path planning based on multi-agent reinforcement learning. *IEEE access*, 7:146264–146272, 2019.

[20] Tabish Rashid, Gregory Farquhar, Bei Peng, and Shimon Whiteson. Weighted qmix: Expanding monotonic value function factorisation for deep multi-agent reinforcement learning. *Advances in Neural Information Processing Systems (NeurIPS)*, 2020.

[21] Tabish Rashid, Mikayel Samvelyan, Christian Schroeder De Witt, Gregory Farquhar, Jakob Foerster, and Shimon Whiteson. QMIX: Monotonic Value Function Factorisation for Deep Multi-Agent Reinforcement Learning. In *International Conference on Machine Learning (ICML)*, 2018.

[22] Mikayel Samvelyan, Tabish Rashid, Christian Schroeder de Witt, Gregory Farquhar, Nantas Nardelli, Tim G. J. Rudner, Chia-Man Hung, Philiph H. S. Torr, Jakob Foerster, and Shimon Whiteson. The StarCraft Multi-Agent Challenge. *arXiv preprint arXiv:1902.04043*, 2019.

[23] Kyunghwan Son, Daewoo Kim, Wan Ju Kang, David Earl Hostallero, and Yung Yi. QTRAN: Learning To Factorize with Transformation for Cooperative Multi-Agent Reinforcement Learning. In *International Conference on Machine Learning (ICML)*, 2019.

[24] Kefan Su and Zongqing Lu. Divergence-Regularized Multi-Agent Actor-Critic. *arXiv preprint arXiv:2110.00304*, 2021.

[25] Peter Sunehag, Guy Lever, Audrunas Gruslys, Wojciech Marian Czarnecki, Vinicius Zambaldi, Max Jaderberg, Marc Lanctot, Nicolas Sonnerat, Joel Z Leibo, Karl Tuyls, et al. Value-Decomposition Networks for Cooperative Multi-Agent Learning Based on Team Reward. In *International Conference on Autonomous Agents and Multiagent Systems (AAMAS)*, 2018.

[26] Ardi Tampuu, Tambet Matiisen, Dorian Kodelja, Ilya Kuzovkin, Kristjan Korjus, Juhan Aru, Jaan Aru, and Raul Vicente. Multiagent cooperation and competition with deep reinforcement learning. *PloS one*, 12(4):e0172395, 2017.

[27] Ming Tan. Multi-agent reinforcement learning: Independent vs. cooperative agents. In *International Conference on Machine Learning (ICML)*, 1993.

[28] Oriol Vinyals, Igor Babuschkin, Wojciech M Czarnecki, Michaël Mathieu, Andrew Dudzik, Junyoung Chung, David H Choi, Richard Powell, Timo Ewalds, Petko Georgiev, et al. Grandmaster Level in StarCraft II Using Multi-Agent Reinforcement Learning. *Nature*, 575(7782):350–354, 2019.

[29] Jianhao Wang, Zhizhou Ren, Terry Liu, Yang Yu, and Chongjie Zhang. Qplex: Duplex Dueling Multi-Agent Q-Learning. In *International Conference on Learning Representations (ICLR)*, 2021.

[30] Yihan Wang, Beining Han, Tonghan Wang, Heng Dong, and Chongjie Zhang. Dop: Off-policy multi-agent decomposed policy gradients. In *International Conference on Learning Representations (ICLR)*, 2020.

[31] Chao Yu, Akash Velu, Eugene Vinitsky, Yu Wang, Alexandre Bayen, and Yi Wu. The surprising effectiveness of ppo in cooperative, multi-agent games. *arXiv preprint arXiv:2103.01955*, 2021.

[32] Kaiqing Zhang, Zhuoran Yang, and Tamer Başar. Multi-agent reinforcement learning: A selective overview of theories and algorithms. *Handbook of Reinforcement Learning and Control*, pages 321–384, 2021.

[33] Kaiqing Zhang, Zhuoran Yang, Han Liu, Tong Zhang, and Tamer Basar. Fully decentralized multi-agent reinforcement learning with networked agents. In *International Conference on Machine Learning (ICML)*, 2018.

[34] Tianhao Zhang, Yueheng Li, Chen Wang, Guangming Xie, and Zongqing Lu. FOP: Factorizing Optimal Joint Policy of Maximum-Entropy Multi-Agent Reinforcement Learning. In *International Conference on Machine Learning (ICML)*, 2021.

[35] Zhengyuan Zhou, Panayotis Mertikopoulos, Nicholas Bambos, Peter Glynn, and Claire Tomlin. Multi-agent online learning with imperfect information, 2018.

Checklist

1. For all authors...
   (a) Do the main claims made in the abstract and introduction accurately reflect the paper's contributions and scope? [Yes]
   (b) Did you describe the limitations of your work? [Yes] See Section 3.4.
   (c) Did you discuss any potential negative societal impacts of your work? [N/A] As we provide a new method for decentralized MARL, we do not see any potential negative societal impacts at this stage.
   (d) Have you read the ethics review guidelines and ensured that your paper conforms to them? [Yes]
2. If you are including theoretical results...
   (a) Did you state the full set of assumptions of all theoretical results? [Yes] We have clearly stated the assumptions in Section 3.2 and 3.3, and further discussed them in Section 3.4.
   (b) Did you include complete proofs of all theoretical results? [Yes] We include the proof of Theorem 1 in Section 3.2, and include the proofs of Theorem 2,3,4 in Appendix A.
3. If you ran experiments...
   (a) Did you include the code, data, and instructions needed to reproduce the main experimental results (either in the supplemental material or as a URL)? [Yes]
   (b) Did you specify all the training details (e.g., data splits, hyperparameters, how they were chosen)? [Yes] We include the training details in Appendix C.
   (c) Did you report error bars (e.g., with respect to the random seed after running experiments multiple times)? [Yes]
   (d) Did you include the total amount of compute and the type of resources used (e.g., type of GPUs, internal cluster, or cloud provider)? [Yes] We include the details of computation in Appendix C.
4. If you are using existing assets (e.g., code, data, models) or curating/releasing new assets...
   (a) If your work uses existing assets, did you cite the creators? [Yes]
   (b) Did you mention the license of the assets? [Yes]
   (c) Did you include any new assets either in the supplemental material or as a URL?[Yes]
   (d) Did you discuss whether and how consent was obtained from people whose data you're using/curating? [N/A] We do not use any dataset in this paper.
   (e) Did you discuss whether the data you are using/curating contains personally identifiable information or offensive content? [N/A]
5. If you used crowdsourcing or conducted research with human subjects...
   (a) Did you include the full text of instructions given to participants and screenshots, if applicable? [N/A]
   (b) Did you describe any potential participant risks, with links to Institutional Review Board (IRB) approvals, if applicable? [N/A]
   (c) Did you include the estimated hourly wage paid to participants and the total amount spent on participant compensation? [N/A]

A Proof

Theorem 2. *In deterministic environments, all agents will converge to the optimal policies, if each agent i performs Q-learning on the transition function $s'^* = \arg\max_{s' \in \mathcal{N}(s,a_i)} Q_i^{\text{ss}}(s, s')$.*

Proof. According to Theorem 1, we know that if each agent i performs Q-learning on ideal transition function, all agents will converge to the global optimal policies. Therefore, to prove Theorem 2 is to prove that $s'^* = \arg\max_{s' \in \mathcal{N}(s,a_i)} Q_i^{\text{ss}}(s, s')$ is a transition function under one of the optimal conditional joint policies of other agents $\boldsymbol{\pi}^*_{-i}(s, a_i)$. Since

$$Q(s, \boldsymbol{a}) = Q(s, a_i, \boldsymbol{a}_{-i}) = r(s, s') + \gamma \max_{\boldsymbol{a}'} Q(s', \boldsymbol{a}'),$$

where s' is the deterministic next state of $\boldsymbol{a}_{-i}$ when given s and a_i, according to (10), we have

$$Q(s, a_i, \boldsymbol{a}_{-i}) = r(s, s') + \gamma \max_{\boldsymbol{a}'} Q(s', \boldsymbol{a}') = r(s, s') + \gamma \max_{s''} Q_i^{\text{ss}}(s', s'') = Q_i^{\text{ss}}(s, s').$$

Thus, $\max_{s'} Q_i^{\text{ss}}(s, s') = \max_{\boldsymbol{a}_{-i}} Q(s, a_i, \boldsymbol{a}_{-i})$, which means $Q_i^{\text{ss}}(s, s'^*) = Q(s, a_i, \boldsymbol{\pi}^*_{-i}(s, a_i))$. Therefore, when there are multiple $s'^* = \arg\max_{s' \in \mathcal{N}(s,a_i)} Q_i^{\text{ss}}(s, s')$, any one of them is an ideal transition function under one of the optimal conditional joint policies of other agents, and Theorem 2 holds. □

Theorem 3. $\left\|Q_i^{sto} - Q_i\right\|_\infty \leq \frac{\Delta r}{1-\gamma} \left\| \frac{1 - P_{\text{env}}\left(s'^* | s, a_i, \boldsymbol{\pi}^*_{-i}(s, a_i)\right)}{1 - \gamma P_{\text{env}}\left(s'^* | s, a_i, \boldsymbol{\pi}^*_{-i}(s, a_i)\right))} \right\|_\infty$, *where* $\Delta r = r_{\max} - r_{\min}$.

Proof.

$$\begin{aligned}
&\left\|Q_i^{sto} - Q_i\right\|_\infty \\
&= \max_{s, a_i} \left| \sum_{s'} P_{\text{env}}\left(s' | s, a_i, \boldsymbol{\pi}^*_{-i}(s, a_i)\right) \left[r(s, s') + \gamma \max_{a'_i} Q_i^{sto}(s', a'_i) \right] - r(s, s'^*) - \gamma \max_{a'_i} Q_i(s'^*, a'_i) \right| \\
&\leq \max_{s, a_i} \sum_{s' \neq s'^*} P_{\text{env}}\left(s' | s, a_i, \boldsymbol{\pi}^*_{-i}(s, a_i)\right) \left| r(s, s') - r(s, s'^*) \right| \\
&\quad + \gamma \sum_{s' \neq s'^*} P_{\text{env}}\left(s' | s, a_i, \boldsymbol{\pi}^*_{-i}(s, a_i)\right) \left| \max_{a'_i} Q_i^{sto}(s', a'_i) - \max_{a'_i} Q_i(s'^*, a'_i) \right| \\
&\quad + \gamma P_{\text{env}}\left(s'^* | s, a_i, \boldsymbol{\pi}^*_{-i}(s, a_i)\right) \max_{a'_i} \left| Q_i^{sto}(s'^*, a'_i) - Q_i(s'^*, a'_i) \right| \\
&\leq \max_{s, a_i} \left(1 - P_{\text{env}}\left(s'^* | s, a_i, \boldsymbol{\pi}^*_{-i}(s, a_i)\right)\right) \left(\Delta r + \gamma \frac{\Delta r}{1 - \gamma}\right) + \gamma P_{\text{env}}\left(s'^* | s, a_i, \boldsymbol{\pi}^*_{-i}(s, a_i)\right) \left\|Q_i^{sto} - Q_i\right\|_\infty .
\end{aligned}$$

Therefore, we have

$$\left\|Q_i^{sto} - Q_i\right\|_\infty \leq \frac{\Delta r}{1 - \gamma} \left\| \frac{1 - P_{\text{env}}\left(s'^* | s, a_i, \boldsymbol{\pi}^*_{-i}(s, a_i)\right)}{1 - \gamma P_{\text{env}}\left(s'^* | s, a_i, \boldsymbol{\pi}^*_{-i}(s, a_i)\right))} \right\|_\infty .$$

□

The bound in Theorem 3 show that Q_i of I2Q is closer to the true value if the transition probability of s'^* is higher in stochastic environments. Since we sample transitions from $\mathcal{D}_i$ to update f_i by maximizing (12):

$$\mathbb{E}_{s, a_i, s' \sim \mathcal{D}_i} \left[\lambda Q_i^{\text{ss}}(s, f_i(s, a_i)) - (f_i(s, a_i) - s')^2 \right],$$

the second term makes the predicted next state $f_i(s, a_i)$ be close to the ***high-frequency*** next states given s and a_i in replay buffer $\mathcal{D}_i$, which means that the transition probability of the predicted next state $P_{\text{env}}\left(f_i(s, a_i) | s, a_i, \boldsymbol{\pi}^*_{-i}(s, a_i)\right)$ would not be too small. Thus, Q_i of I2Q will be close to the true value and the worst cases where the predicted next states have very small transition probabilities can be avoided according to our implementation (12). ***That is the reason why I2Q can be successfully applied in stochastic environments***, as shown in Figure 8 and Figure 10.

Theorem 4. *$Q_i^o(s, a_i)$ is the value function learned on the ideal transition function $s'^o = f_i^o(s, a_i)$, $Q_i(s, a_i)$ is the value function learned on the modeled ideal transition function $s' = f_i(s, a_i)$, considering the continues state space, $\|Q_i^o - Q_i\|_\infty \leq \frac{T+\gamma G}{1-\gamma} \|f_i^o - f_i\|_\infty$, where $G = \max_{s,a} |\frac{\partial Q_i(s,a)}{\partial s}|, T = \max_{s,s'} |\frac{\partial r(s,s')}{\partial s'}|$, when $f_i(s, a_i)$ is close to $f_i^o(s, a_i)$.*

Proof.

$$
\begin{aligned}
&\|Q_i^o - Q_i\|_\infty \\
&= \max_{s,a} \left| r(s, s'^o) + \gamma \max_{a_i'} Q_i^o(s'^o, a_i') - r(s, s') - \gamma \max_{a_i'} Q_i(s', a_i') \right| \\
&\leq \max_{s,a} \left| r(s, s'^o) - r(s, s') \right| + \gamma \left| \max_{a_i'} Q_i^o(s'^o, a_i') - \max_{a_i'} Q_i(s', a_i') \right| \\
&= \max_{s,a} \left| \frac{\partial r(s, s'^o)}{s'^o}(s' - s'^o) + o(s' - s'^o) \right| \\
&\quad + \gamma \left| \max_{a_i'} Q_i^o(s'^o, a_i') - \max_{a_i'} [Q_i(s'^o, a_i') - \frac{\partial Q_i(s'^o, a_i')}{s'^o}(s' - s'^o) - o(s' - s'^o)] \right| \\
&\leq \max_{s,s'} \left| \frac{\partial r(s, s')}{\partial s'} \right| \max \left| s' - s'^o \right| + \gamma \max_{s,a_i} |Q_i^o(s, a_i) - Q_i(s, a_i)| + \gamma \max_{s,a} |\frac{\partial Q_i(s, a)}{\partial s}| \max \left| s' - s'^o \right| + o(s' - s'^o) \\
&= \gamma \|Q_i^o - Q_i\|_\infty + (T + \gamma G) \|f_i^o - f_i\|_\infty + o(\|f_i^o - f_i\|_\infty).
\end{aligned}
$$

Omiting the remainder term, we have

$$
\|Q_i^o - Q_i\|_\infty \leq \frac{T + \gamma G}{1 - \gamma} \|f_i^o - f_i\|_\infty .
$$

□

Theorem 4 shows that the difference between ideal values Q_i^o and learned values Q_i is bounded by the error of modeled transition function. As shown in Figure 5, the learned values of I2Q are very close to the ideal values, because I2Q accurately models the ideal transition function.

B Additional Results

B.1 Hyperparameter λ

In Section 4.2, we have shown the effectiveness of λ. Here, we further discuss the cases where $\lambda = 0$. When $\lambda = 0$, I2Q degenerates into a popular model-based method MBPO [9]. In existing model-based methods, the modeled transition functions follow the transition probabilities in the replay buffer, which are non-stationary and outdated, so existing model-based methods also face the non-stationary problem. As shown in Figure 7 and Figure 11, I2Q outperforms I2Q with $\lambda = 0$, which verifies the effectiveness of the proposed objective function of the transition function f_i in I2Q.

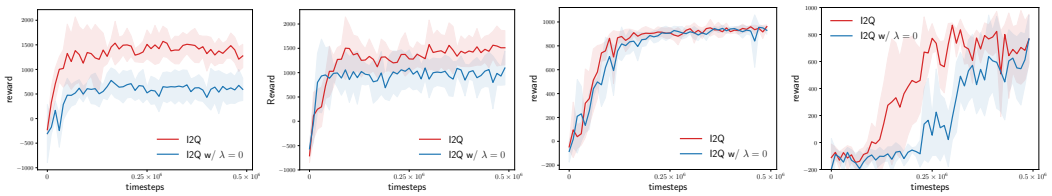

(a) 2×3 HalfCheetah (b) $2|4$ HalfCheetah (c) 2×4 Ant (d) $6|2$ Ant

Figure 11: Learning curves with $\lambda = 0$.

B.2 Two Update Rules

We propose two update rules for Q_i: rule 1 (14) and rule 2 (15). Figure 12 shows that the two rules achieve similar performance, especially in the tasks with long horizons where the reward of one timestep is insignificant compared with the cumulated return value. We use rule 2 in differential games and use rule 1 in SMAC and Multi-Agent MuJoCo.

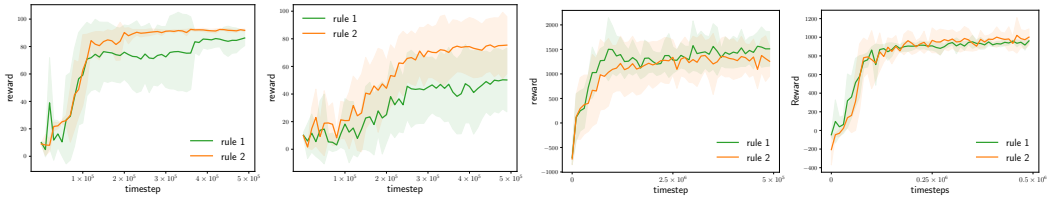

(a) MPE, $N = 2$ (b) MPE, $N = 3$ (c) 2|4 HalfCheetah (d) 2×4 Ant

Figure 12: Learning curves of two update rules.

B.3 Independent PPO

Independent PPO (IPPO) [4] is a strong on-policy decentralized MARL baseline. However, it is not fair to compare off-policy algorithms with on-policy algorithms, since on-policy algorithms do not use old data, which makes them weaker on sample efficiency [1], as shown in Figure 13.

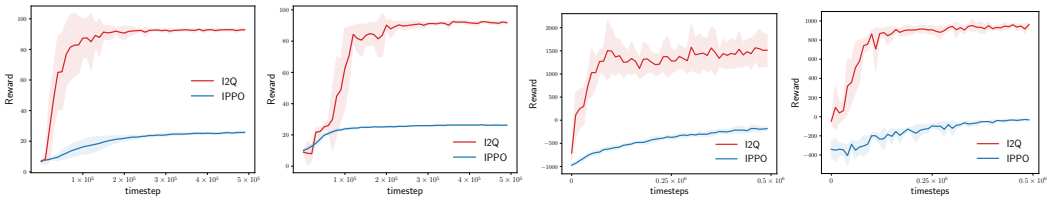

(a) MPE, $N = 2$ (b) MPE, $N = 3$ (c) 2|4 HalfCheetah (d) 2×4 Ant

Figure 13: Learning curves of IPPO.

B.4 Scalability

We test I2Q on 6-agent Walker and 8-agent Ant with full observation setting, the results are shown in Figure 14. Taking state information as input, IDDPG is strong enough, but I2Q can still obtain performance gain on 8-agent Ant.

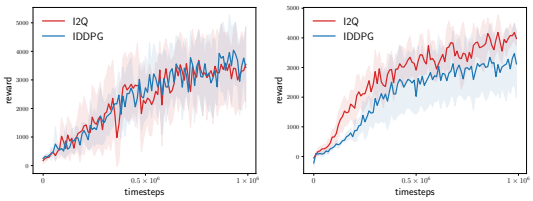

(a) 6×1 Walker (b) 8×1 Ant

Figure 14: Learning curves on Multi-Agent MuJoCo.

B.5 Multiple Optimal Joint Policies

In Section 3.4, we have analyzed that I2Q can easily solve the task with multiple optimal joint policies. Here, we give another way to solve this problem. When agent i selects one of the optimal independent action, the neighboring state set $\mathcal{N}(s, a_i)$ contains one of the optimal next states, which have the max $Q_i^{\text{SS}}(s, s')$. The union of the neighboring state sets $\cap_i \mathcal{N}(s, a_i)$ is a singleton set, which contains the next state of the joint action. If each $\mathcal{N}(s, a_i)$ contains different optimal next states, the union $\cap_i \mathcal{N}(s, a_i)$ might contain none of the optimal ones. We let each agent independently and randomly initialize a same fixed noise function $\eta(s)$, using the same random seed, as a partial order, and makes decisions by the partial order

$$\arg\max_{a_i^*} \eta(s'^*), \quad s'^* = \arg\max_{s' \in N(s, a_i^*)} Q_i^{\text{SS}}(s, s').$$

Thus, each $\mathcal{N}(s, a_i)$ will contain the optimal next state with the max η value, which is the next state of the joint action. Thus, the agents are coordinated by η. Since the noise function η is randomly initialized, it is a small probability event to find multiple next states with the same η value. We could also adopt other partial orders, *e.g.*, l_1 norm of s'.

We test I2Q on a one-stage matrix game with two optimal joint policies $(1, 2)$ and $(2, 1)$, as shown in Figure 15. If the agents independently select actions, they might choose the miscoordinated joint policies $(1, 1)$ and $(2, 2)$. IQL learns the suboptimal policy $(1, 1)$, but I2Q agents always select coordinated actions, though the value gap between the optimal policy and suboptimal policy is so small.

a_2 \ a_1	$\mathcal{A}^{(1)}$	$\mathcal{A}^{(2)}$	$\mathcal{A}^{(3)}$
$\mathcal{A}^{(1)}$	9.99	**10**	0
$\mathcal{A}^{(2)}$	**10**	0	0
$\mathcal{A}^{(3)}$	0	0	0

(a) matrix game

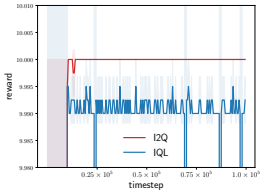

(b) learning curves

Figure 15: Learning curves on a one-stage matrix game with multiple optimal joint policies.

B.6 Discussion on D3G

D3G predicts the optimal next state s'^* with the highest QSS value and decodes actions in execution by training a inverse model $a_i = g(s, s'^*)$. Different from D3G, I2Q builds transition function $f_i(s, a_i)$ using QSS value and trains Q-learning on $f_i(s, a_i)$. Several drawbacks limit the performance of D3G in decentralized MARL. First, over-generalization of $g(s, s'^*)$ would lead to wrong a_i. Considering two inverse maps $(s, s'^1) \to a^1$ and $(s, s'^2) \to a^2$, where s'^1 and s'^2 are very similar but a^1 and a^2 are very different, which is common in complex continuous environments, trained by supervised learning, the inverse model g may *mistakenly* predict $g(s, s'^1)$ as the average of a^1 and a^2, due to the generalization of neural network on state space. Since a^1 and a^2 are very different, the prediction error is large and leads to poor performance. Experimentally, we find it is hard to perfectly train the inverse model $g(s, s')$, and the prediction error of actions greatly influences the performance in practice. I2Q could avoid this problem since it learns accurate values $Q_i(s, a^1)$ and $Q_i(s, a^2)$ and selects the action with the highest value. Second, as stated in the experiment section, the implementation of D3G adopts a forward model, which requires the transition probabilities in replay buffer $\mathcal{D}_i$ to be deterministic, which is impossible in decentralized MARL. The motivation and implementation of I2Q are very different from that of D3G, which makes I2Q more suitable and practical in decentralized MARL, as shown in Figure 6 and Figure 9. The original D3G can only be used in continuous action space, and we extend it to discrete space and compare it in SMAC. Due to the analyzed drawbacks, discrete D3G cannot obtain a winning rate in SMAC, as shown in Table 1.

Table 1: Winning rate on SMAC.

	8m	3s_vs_4z	2s3z	5m_vs_6m
I2Q	89%	68%	85%	42%
discrete D3G	0	0	0	0

B.7 I2Q without Forward Model

For practicability, we design an approximation of I2Q without forward model f_i, which is enlightened by implicit Q-learning[11]. Implicit Q-learning learns the optimal value without predicting next actions, similarly, we can obtain QSS value without predicting next states. Following Implicit Q-learning, we introduce $V_i(s)$ and utilize expectile regression. Specifically, we update Q_i^{ss} by minimizing

$$\mathbb{E}_{s,s',r\sim\mathcal{D}_i}[(Q_i^{\text{ss}}(s, s') - r - \gamma V_i(s'))^2],$$

update $V_i(s')$ by minimizing expectile loss

$$\mathbb{E}_{s,s'\sim\mathcal{D}_i}[L_2^\tau(Q_i^{\text{ss}}(s, s') - V_i(s'))], \quad L_2^\tau(u) = |\tau - 1(u < 0)|u^2.$$

Using the approximate QSS value, we have

$$Q_i^{\text{ss}}(s, s'^*) = \max_{s'\in\mathcal{N}(s,a_i)} Q_i^{\text{ss}}(s, s')$$

According to Eq 15 and the mathematical derivation between line 161 and line 162, we update $Q_i(s, a_i)$ to be $Q_i^{\text{ss}}(s, s'^*)$ by minimizing

$$\mathbb{E}_{s,a_i,s' \sim \mathcal{D}_i}[(Q_i(s, a_i) - \max(\bar{Q}_i(s, a_i), \bar{Q}_i^{\text{ss}}(s, s')))^2].$$

Although QSS value is a biased estimation in this implementation, the implementation without forward model is practical. We test I2Q w/o forward model in SMAC. The results are shown in Figure 16. I2Q w/o f shows similar performance with I2Q, and does not need to learn the forward model, thus it would be more practical in complex environments.

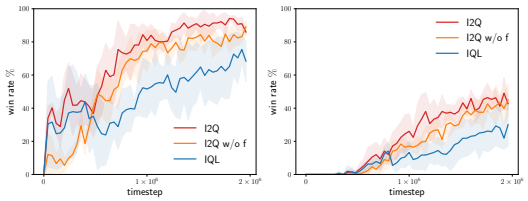

(a) 2s3z (b) 5m_vs_6m

Figure 16: Learning curves on SMAC.

C Hyperparameters

In 2×3 HalfCheetah, there are two agents and each of them controls 3 joints of HalfCheetah. In $2|4$ HalfCheetah, there are two agents. One of them controls 2 joints, and one of them controls 4 joints. And so on.

In MPE-based (MIT license) differential games and Multi-Agent MuJoCo (MIT license), we adopt the implementation of SpinningUp [1] (MIT license), the SOTA implementation of DDPG, and follow all hyperparameters in SpinningUp. The discount factor $\gamma = 0.99$, the learning rate is 0.001 with Adam optimizer, the batch size is 100, the replay buffer contains 1×10^6 transitions, the hidden units are 256.

In SMAC (MIT license), we adopt the implementation of PyMARL [22] (Apache-2.0 license) and follow all hyperparameters in PyMARL. The discount factor $\gamma = 0.99$, the learning rate is 0.0005 with RMSprop optimizer, the batch size is 32 episodes, the replay buffer contains 5000 episodes, the hidden units are 64. We adopt the version SC2.4.10.

The hyperparameter λ has been fully tested in MPE-based differential games. In Multi-Agent MuJoCo, we set $\lambda = 0.01$, and in SMAC, we set $\lambda = 0.05$.

The experiments are carried out on Intel i7-8700 CPU and NVIDIA GTX 1080Ti GPU. The training of each MPE and Multi-Agent MuJoCo task could be finished in 5 hours, and the training of each SMAC task could be finished in 20 hours.